SenSation : A New Translational 2 DOF Haptic Device with Parallel Mechanism

Young-Hoon Chung and Jae-Won Lee

Abstract: We propose a new two-degree of freedom parallel mechanism for a haptic device and will refer to the mechanism as the *SenSation*. The *SenSation* is designed in order to improve the kinematic performance and to achieve static balance. We use the pantograph mechanisms in order to change the location of active joints, which leads to transform a direct kinematic singularity into a non-singularity. The direct kinematic singular configurations of the *SenSation* occur near the workspace boundary. Using the property that position vector of rigid body rotating about a fixed point is normal to the velocity vector, Jacobian matrix is derived. Using the vector method, two different types of singularities of the SenSation can be identified and we discuss the physical significance of each of the three types of singularities. We will compare the kinematic performances(force manipulability ellipsoid, kinematic isotropy) of the *SenSation* with those of five-bar parallel mechanism. By specifying that the potential energy be fixed, the conditions for the static balancing of the *SenSation* is derived. The static balancing is accomplished by changing the center of mass of the links.

Keywords: parallel mechanism, haptic device, kinematic isotropy, manipulability ellipsoid, singularity, static balance

I. Introduction

Recently, one interesting application in robotics research is the haptic device. A haptic device is the machinery that is designed to provide user with a sense of touch. The device is essentially a robotic arm that is able to both sense its pose at that location and apply a force at that location. A user can take hold of the end-effector of the device and, by means of the use of haptic control algorithm, feel as if he/she is actually touching and interacting with the virtual model or remote site.

The force supplied by the device provides instantaneous and intuitive feedback on the task being performed. The haptic device must not distort the reflected forces by its mechanical characteristics. To provide user with a precise sense of touch, the haptic device should be able to have performances such as low apparent mass /inertia, high structural stiffness, wide singular-free workspace, static balancing(or counterbalancing), high force bandwidth, backdriveability, very low friction and backlash, high force dynamic range, good transportability [1][2][3]. These demands are often conflicting and difficult to achieve.

It can be seen that parallel mechanisms are suitable for structure of haptic device because they have a number of advantages such as high structural stiffness and force bandwidth, low inertia. Other demands can be achieved through the use of haptic control. The haptic device with parallel mechanism is in [4]-[11]

The kinematic isotropy is very important since it leads to a high stiffness and force bandwidth, wide singular-free isotropic workspace, a good position and orientation accuracy. Unfortunately, typical serial and parallel mechanisms have not constant high stiffness and force bandwidth over the entire workspace. The reason is that the isotropy performance tends to be degraded as the mechanism goes to near singular configurations. There are three types of singular configu-rations in parallel mechanisms: direct kinematic singularity (DKS), inverse kinematic singularity(IKS)[12][13], architecture singularity (AS)[14]. The DKS, one of three singularities, exists inside of workspace and separates its workspace into a number of regions. Therefore, the workspace of parallel mechanisms becomes small compared to link size.

To deal with this singularity(DKS) and improve the kinematic isotropy, [15] and [16] had proposed the method of actuator redundancy. [17] used the method to eliminate this type singularity. [6] also added one actuator to obtain a more symmetrical workspace and more force of end-effector. However, this method makes a controller design complex.

[18] proposed method eliminating the DKS by applying additional constraint to the mechanism.

In general, the optimization of link parameters has been used to improve the isotropy of parallel mechanisms [5,8]. Cost functions have been proposed to describe kinematic isotropy, manipulability and accuracy. However, this optimization can't vary the two types of a singular configuration of mechanisms(DKS, IKS).

For a haptic device, a very interesting mechanism having tendon transmission in order to drive the 5-bar linkage was proposed in [7]. They improved kinematic isotropy by optimizing the radius of guide pulleys. From the paper, I found out the fact that, although the mechanism has two actuators for 2 DOF, the mechanism has the effect equivalent to actuator redundancy since four different wrench screws form the matrix of rank 2 under a non-singular configuration.

In this paper, we propose a translational 2-DOF haptic device, the *SenSation*, having parallel mechanism. The *SenSation* is designed in order to improve kinematic performance such as wide a singular-free workspace, a good kinematic isotropy through the entire workspace, and to achieve static balancing. These performances can be achieved by using adopting pantograph mechanisms as each leg without the actuator redundancy and the optimization of link parameters. We prove that the *SenSation* has both wide a singular-free workspace and a good kinematic isotropy all over its workspace by illustrating a force manipulability ellipsoid and the singularity loci.

Manuscript received: Aug. 31, 2001., Accepted: Nov. 19, 2001
Young-Hoon Chung: Robotics Lab., Graduate School of Mech. Eng. Yeungnam University, Gyoung-San, Korea (haptics@hanmail.net)
Jae-Won Lee: School of Mechanical Engineering Yeungnam University, Gyoung-San, Korea. (jwlee@yu.ac.kr)

II. Description of the *sensation*

The *SenSation* consists of two pantograph mechanisms. The joint **a*** and **c*** is attached to the link **AB** and **CD** respectively, and the joint **A** and **C** is attached to the link **AE** and **CG** respectively. The distance between joint **A** and **C** is d. The global fixed coordinate frame{**O**} is located at point O. The output is the joint **P** as shown in Fig.1.

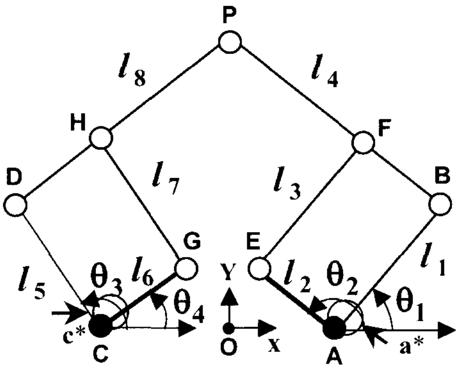

Fig. 1. Schematic diagram and its coordinate system.

Two motors are attached to the joint **A** of link **AE** and **C** of link **CG** respectively. When input links **AE** and **CG** rotate about joint **A** and **C** respectively, the links **BP** and **DP** have also the same rotation angle. Therefore, the joint **B** and **D** are also active joints, which lead to transform the direct kinematic singular configuration into non-singular one. The *SenSation* has translational two-degree of freedom, as can be shown by applying the mobility criterion presented in Hunt[20]:

$$M = 3(n - j - 1) + \sum_{i=1}^{j} f_i \tag{1}$$

where M is the degree of freedom of mechanisms, n is the number of bodies in the mechanism, j is the number of joints and f_i is the number of degree of freedom of i-th joint.
For the *SenSation*, $n=9, j=11$ and $f_i=1$ for each of the revolute joints. Application of Eq. (1) yields

$$M = 3(9-11-1)+11 = 2 \tag{2}$$

III. Kinematic analysis

1. Inverse Kinematics

For the inverse kinematics, P_x, P_y are given, and the active joint angles θ_2, θ_4 ,are to be found. This can be can be accomplished on a sub-chain(**O→C→D→P**) by sub-chain (**O→A→B→P**). Figure 2 shows the link lengths and joint angles for a right sub-chain(**O→A→B→P**).

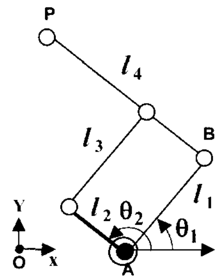

Fig. 2. A right sub-chain of the *SenSation*.

From the geometry of Fig. 2, a vector-loop equation can be written as

$$\overrightarrow{OP} = \overrightarrow{OA} + \overrightarrow{AB} + \overrightarrow{BP} \tag{3}$$

Expressing the vector-loop equation above in the global fixed coordinate frame{**O**} gives

$$\begin{aligned} P_x &= \frac{d}{2} + l_1 C_1 + l_4 C_2 \\ P_y &= 0 + l_1 S_1 + l_4 S_2 \end{aligned} \tag{4}$$

Since θ_1 is a passive joint angle, it should be eliminated from the equation (4). Toward this goal, we write Eq. (4) in the following form:

$$\begin{aligned} P_x - (\frac{d}{2} + l_4 C_2) &= l_1 C_1 \\ P_y - l_4 S_2 &= l_1 S_1 \end{aligned} \tag{5}$$

Summing the squares of two equations in (5) yields

$$(P_x - d/2 - l_4 C_2)^2 + (P_y - l_4 S_2)^2 - l_1^2 = 0 \tag{6}$$

We can arrange Eq.(6) in the following form:

$$\alpha_1 C_2 + \beta_1 S_2 + \lambda_1 = 0 \tag{7}$$

where, $\alpha_1 = -2(P_x - d/2)l_4$, $\beta_1 = 2P_y l_4$,

$$\gamma_1 = (P_x - d/2)^2 + P_y^2 + l_4^2 - l_1^2$$

Substituting the trigonometric identities

$$\mathbf{cos}(\theta_2) = \frac{1-u_1^2}{1+u_1^2}, \mathbf{sin}(\theta_2) = \frac{2u_1}{1+u_1^2}, \text{ where, } \mathbf{tan}\left(\frac{\theta_2}{2}\right) = u_1$$

into Eq.(7), we obtain

$$(\gamma_1 - \alpha_1)u_1^2 + 2\beta_1 u_1 + (\gamma_1 + \alpha_1) = 0 \tag{8}$$

Solving Eq.(8) for u_1 yields

$$u_1 = \frac{-\beta_1 \pm \sqrt{\beta_1^2 - (\gamma_1^2 - \alpha_1^2)}}{\gamma_1 - \alpha_1} \tag{9}$$

, and then

$$\theta_2 = 2\mathbf{tan}^{-1}\left(\frac{-\beta_1 \pm \sqrt{\beta_1^2 - (\gamma_1^2 - \alpha_1^2)}}{\gamma_1 - \alpha_1}\right) \tag{10}$$

Hence, corresponding to each given point **P** location, there are generally two solutions of θ_2 and two configurations of a right sub-chain. When Eq.(8) yields a double root, the two links **AB** and **BP** are in a fully stretched-out or folded-back configuration called the singular configuration. When Eq.(8) yields no real root, the specified point **P** location is not reachable. Following the same procedure, another sub-chain(O→C→D→P). configuration can be solved. We conclude that, in general, there are a total of four possible postures corresponding to a given point P location.

2. Jacobian Matrix

The input vector is $\vec{\theta}_a = [\theta_2, \theta_4]^T$ and the output vector $\overrightarrow{OP} = [P_x, P_y]^T$. A loop-closure equation can be written for each sub-chain. For a right sub-chain, we have

$$\overrightarrow{OP} = \overrightarrow{OA} + \overrightarrow{AB} + \overrightarrow{BP} \tag{11}$$

The angular velocity vectors of all links point in the positive z-direction as shown in Fig.1. A velocity vector- loop equation is obtained by taking the derivative of Eq.(11) with respect to time:

$$\dot{\overrightarrow{OP}} = \dot{\theta}_1 \vec{k} \times \overrightarrow{AB} + \dot{\theta}_2 \vec{k} \times \overrightarrow{BP} \tag{12}$$

where $\vec{k}$ is a unit vector pointing in the positive z-axis direction. Since $\dot{\theta}_1$ is a passive variable, it should be eliminated from Eq.(12). To achieve this goal, we use the fact that the position vector of the rigid body rotating about a fixed point is normal to the velocity vector. We dot-multiply both sides of Eq.(12) by $\overrightarrow{AB}$, which leads to

$$\overrightarrow{AB} \bullet \dot{\overrightarrow{OP}} = \dot{\theta}_2 \vec{k} \bullet \left(\overrightarrow{BP} \times \overrightarrow{AB}\right) \tag{13}$$

Following the same procedure like Eq.(11),(12) and (13), for a left(**O→C→D→P**) sub-chain, yields

$$\overrightarrow{CD} \bullet \dot{\overrightarrow{OP}} = \dot{\theta}_4 \vec{k} \bullet \left(\overrightarrow{DP} \times \overrightarrow{CD}\right) \tag{14}$$

Eq.(13) and (14) can be arranged in matrix form :

$$J_p \dot{\overrightarrow{OP}} = J_\theta \dot{\vec{\theta}}_a \tag{15}$$

$$J_\theta = \begin{bmatrix} \vec{k} \bullet (\overrightarrow{BP} \times \overrightarrow{AB}) & 0 \\ 0 & \vec{k} \bullet (\overrightarrow{DP} \times \overrightarrow{CD}) \end{bmatrix} = \begin{bmatrix} l_1 l_4 S_{1-2} & 0 \\ 0 & l_5 l_8 S_{3-4} \end{bmatrix}$$

$$J_p = \begin{bmatrix} \overrightarrow{AB} & \overrightarrow{CD} \end{bmatrix}^T = \begin{bmatrix} l_1 C_1 & l_1 S_1 \\ l_5 C_3 & l_5 S_3 \end{bmatrix}, \quad S_{i-j} = sin(\theta_i - \theta_j), \; C_{i-j} = cos(\theta_i - \theta_j)$$

3. Singularity Analysis

By using the method, a great deal of physical insight into the singularity problem is gained, and it is possible to determine the workspace easily.

We also discuss the physical significance of each of the two types of singularities. Due to the existence of two Jacobian matrices, a parallel mechanism or manipulator is said to be at a singular configuration when either J_θ or J_p or both are singular[12].

3.1 Direct Kinematic Singularities(DKS)

The direct kinematic singularity(DKS) arise when J_p, in Eq.(15), is singular, i.e., Det(J_p) = 0 .

$$\left| \overrightarrow{AB} \;\; \overrightarrow{CD} \right| = 0 \tag{16}$$

Geometrically, this means that the vector $\overrightarrow{AB}$ parallels the vector $\overrightarrow{CD}$ (Fig.3). Therefore, the vector $\overrightarrow{AB}$ and $\overrightarrow{CD}$ form a linearly dependent set of rank 1. This type of direct kinematic singularity is shown in Fig.3.

In Eq.(15), there exist some nonzero vector $\dot{\vec{P}}$ vectors that result in zero $\dot{\vec{\theta}}_a$ vectors if J_p is singular. That is, the output **P** can possess infinitesimal motion in some direction while all the actuators are completely locked. Hence, the point **P** gains additional one degree of freedom and it cannot withstand external force along the directions that are perpendicular to $\overrightarrow{AB}$ (or $\overrightarrow{CD}$) at **P** (see Fig.3.).

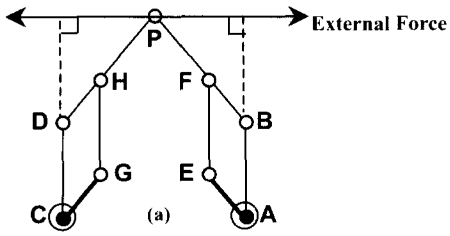

Fig. 3. Direct kinematic singular configuration.

In typical parallel mechanism, direct kinematic singularities usually exist in the inside of the workspace and this is important one of the disadvantages that typical parallel mechanisms have. For overcoming this singularity problem, the Hexel machine have 8-motor for 5 axis use and Coline.C.L[15], S.J.Ryu and J.W.Kim and F.C.Park[17] have added actuators. However, we overcame this problem by changing only the location of actuation whitout adding actuators because we design the *Sensation* so that the direct kinematic singularity(**DKS**) occurs near the workspace boundary as shown in Fig.6. It is noticeable.

3.2 Inverse Kinematic Singularities(IKS)

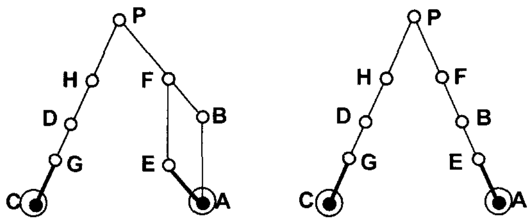

Fig. 4. Inverse kinematic singular configurations.

Inverse kinematic singularity(IKS) of the *SenSation* occurs when the determinant of J_θ go to zero, i.e., Det(J_θ) = 0.

$$\begin{vmatrix} \vec{k} \bullet (\overrightarrow{BP} \times \overrightarrow{AB}) & 0 \\ 0 & \vec{k} \bullet (\overrightarrow{DP} \times \overrightarrow{CD}) \end{vmatrix} = 0 \tag{17}$$

Geometrically, this means that the vector $\overrightarrow{BP}$ parallels $\overrightarrow{AB}$ or $\overrightarrow{DP}$ parallels $\overrightarrow{CD}$. That is, any sub-chain is in a fully stretched-out configuration. This type of inverse kinematic singularity is shown in Fig.4.

When J_θ, in Eq.(15), is singular there exist some nonzero $\dot{\vec{\theta}}_a$ vector that result in zero $\dot{\vec{P}}$ vectors, i.e., infinitesimal rotation of the input link AE and CG result in no output motion of joint **P**. Hence the *SenSation* loses one degree of freedom and can withstand external forces in directions along $\overrightarrow{PA}$ or $\overrightarrow{PC}$ without having actuator torques of joint A and C. In typical parallel mechanism, inverse kinematic singularities usually occur at the workspace boundary. Inverse kinematic singularities of the *SenSation* also occur at the workspace boundary as shown in Fig.6.

IV. Kinematic performance

Since the workspace is separated by the direct kinematic singularities that exist in the inside of workspace, the workspace of typical parallel mechanisms is small.

To compare the singularity locus and workspace of the *SenSation* with those of the five-bar parallel mechanism[15], the direct kinematic singularity(DKS) and inverse kinematic singularity(IKS) loci of both five-bar parallel mechanism and the *SenSation* are shown in Fig.5 and 6 respectively.

Figure 5 represents the singularity and workspace of the five bar mechanism. The workspace is separated by DKS locus which occur at the inside of workspace. Therefore one of the separated areas should be selected for tasks such as path plan. However, we know that the direct kinematic singularity of the *SenSation* occur near the boundary of workspace as shown in figure 6.

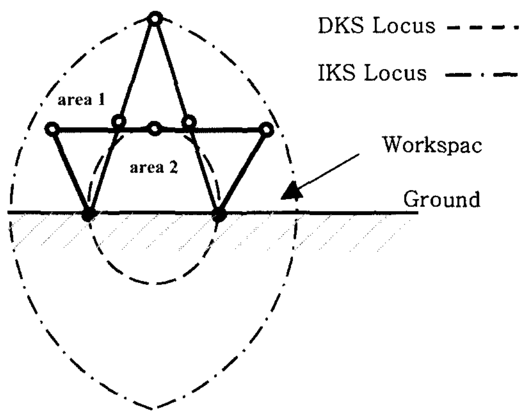

Fig. 5. Singularity and workspace of the five-bar mechanism.

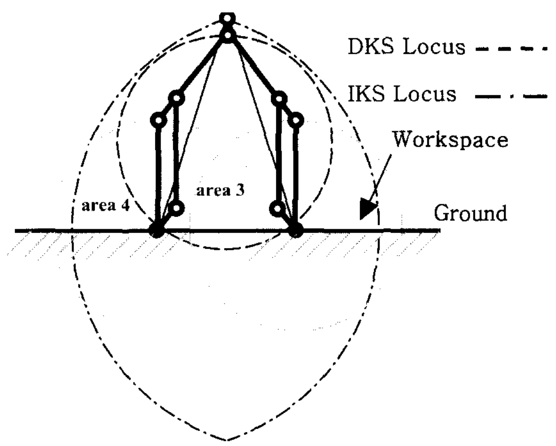

Fig. 6. Singularity and workspace of the *SenSation*.

To compare the kinematic performance of the *SenSation* with that of five-bar parallel mechanism, the manipulability ellipsoid of two mechanisms are represented in Fig.7 and 8.

We select the link parameters of two mechanism, $l_1 = l_5 = l_3 = l_7 = l_4 = l_8 = 0.18$ (m), $l_2 = l_6 = 0.3$ (m), $\mathbf{d} = 0.09$(m) arbitrarily. The manipulability ellipses of the five-bar parallel mechanism are shown in Fig. 7. Because of the direct kinematic singularities at inside of workspace(see Fig.5), the manipulability ellipses is not good. As compared with link size, it has a small workspace.

For the *SenSation*, since there are the direct kinematic singularities near the boundary of workspace(see Fig.6), we know, comparing Fig.5 and 7 with Fig.6 and 8, that this mechanism have the workspace lager than those of five-bar parallel mechanism.

Especially, the improvement in manipulability ellipses from Fig. 7 to Fig. 8 is noticeable. Also, form Fig.8, we know that the *SenSation* have a good the kinematic isotropy through the entire workspace without optimization of the link parameters and adding actuators.

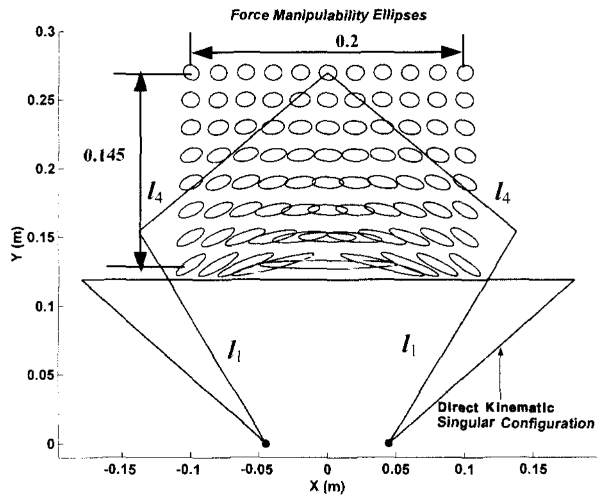

Fig. 7. Manipulability Ellipses of five-bar mechanism.

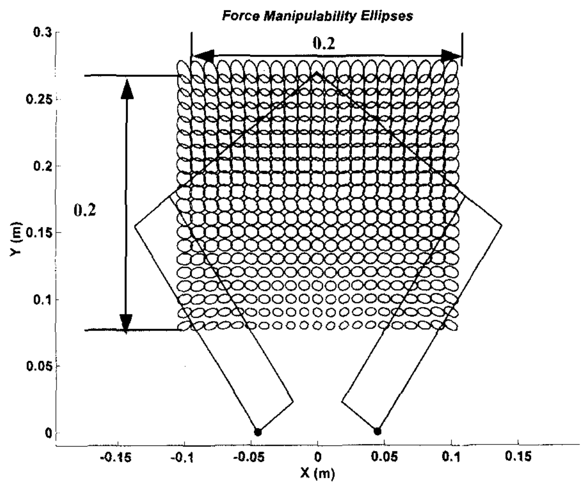

Fig.8. Manipulability Ellipses of the *SenSation*.

V. Static Balance

In the context of manipulators and motion simulation mechanisms, static balancing is defined as the set of conditions under which the weight of the links of the mechanism does not produce any torque at the actuators under static conditions, for any configuration of the mechanism[19]. A balanced mechanism results in better dynamic characteristics and less vibration caused by fast motion. We assume that $l_1 = l_5 = l_3 = l_7$, $l_2 = l_6$, $l_4 = l_8$. The potential energy of the *SenSation* can be written as

$$\begin{aligned} V &= \sum m_i g L_{ci} = g\{m_1 l_{c1} S_1 + m_2 l_{c2} S_2 \\ &+ m_3(l_2 S_2 + l_{c3} S_1) + m_4(l_1 S_1 + l_{c4} S_2) \\ &+ m_1 l_{c1} S_3 + m_2 l_{c2} S_4 \\ &+ m_3(l_2 S_4 + l_{c3} S_3) + m_4(l_1 S_3 + l_{c4} S_4)\} \end{aligned} \tag{18}$$

where m_i is the mass of each link and L_{ci} represents the position of the center of mass of each link.
Rearranging Eq.(18) yields,

$$\begin{aligned} V &= g\{(m_1 l_{c1} + m_3 l_{c3} + m_4 l_1)(S_1 + S_3) \\ &+ (m_2 l_{c2} + m_3 l_2 + m_4 l_{c4})(S_2 + S_4)\} \end{aligned} \tag{19}$$

In Eq. (19), if the coefficients of $(S_1 + S_3)$ and $(S_2 + S_4)$ go to zero, then the potential energy of the *SenSation* will be zero for any configuration. Hence, one obtains the conditions for static balancing as follows

$$\begin{aligned} (m_1 l_{c1} + m_3 l_{c3} + m_4 l_1) = 0 \\ (m_2 l_{c2} + m_3 l_2 + m_4 l_{c4}) = 0 \end{aligned} \tag{20}$$

For satisfying the condition of static balancing described in equation (20), we change the location of center of mass of link 1 and 2. Hence, the static balance of the *SenSation* can be achieved as shown in Fig.9.

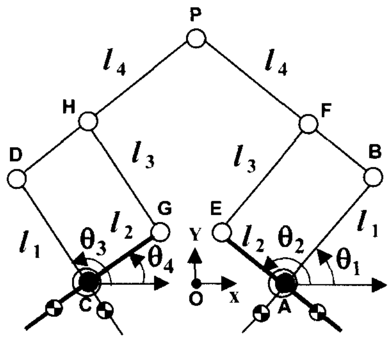

Fig. 9. Static balance of the *SenSation*.

Because the *SenSation* is statically balanced, the actuators are used only to transfer accelerations to the moving links, which leads to a reduction of size and power of the actuators and results in significant improvements of the control and energy efficiency. If the mechanism proposed is applied to the limbs of flight simulator, haptic device, machining center that has the parallel structure, they will have a good dynamic performance.

VI. Conclusion

We proposed a new 2 DOF parallel mechanism that has translational two degrees of freedom. The *SenSation* is designed in order to have not only the global kinematic isotropy performance and static balance.

For the purpose of this kinematic performance, we changed the location of actuations by employing the pantograph mechanism, which result in the existence of direct kinematic singularity locus near the boundary of workspace as shown in Fig.6. Therefore, the *SenSation* overcame disadvantage such as the singular configurations existing in the inside of workspace. Form Fig.8, we knew that the *SenSation* have a good the kinematic isotropy through the entire workspace without optimization of the link parameters and adding actuators. For the purpose of static balance, we derived the condition of zero-potential energy and achieved the static balance by changing the location of center of mass of link 1 and 2 as shown in Fig.9.

Reference

[1] P.A. Millman and J.E. Colgate, "Design of a four degree-of-freedom force reflecting manipulandum with a specified force/torque workspace," *Proc. Of the 1991 IEEE International Conference on Robotics and Automation*, pp. 1488-1493, 1991.

[2] T.H. Massie and J.K. Salisbury, "The Phantom haptic interface: a device for probing virtual objects," *Proc. Of the 1994 ASME Int. Mechanical Engineering Exposition and congress*, pp. 259-301, 1994.

[3] R.R. Ellis, O.M. Ismaeil, and M.G. Lipsett, "Design and evaluation of a high-performance haptic interface," Robotica, vol. 14, pp. 321-327, 1996.

[4] H. Iwata, "Pen-based haptic virtual environment," *Proc. IEEE Virtual Reality Annual International Symposium*, pp. 287-292, 1993.

[5] V. Hayward, L. Choksi, J. Lanvin, and C. Ramstein, "Design and multi-objective optimization of a linkage for a haptic interface," *4th International Workshop on Advances in Robotic Kinematics*, pp. 359-368, 1994.

[6] P. Buttolo and B.Hannaford, "Pen-based force display for precision manipulation in virtual enviroments," *Proc. IEEE Virtual Reality Annual International Symposium*, pp. 217-224, 1995.

[7] G.M.Prisco, A.Frisoli, F.Salsedo, and M.Bergamasco, "A novel tendon driven 5-bar linkage with large isotropic workspace'," *Proc. of the ASME Dynamic Systems and Control Division, International Mechanical Engineering Congress and Exposition (IMECE99), DSC-vol. 67*, pp. 297-304, 1999.

[8] L. Stocco, S.E. Salcudean, and F. Sassani, "Mechanism design for global isotropy with applications to haptic interfaces," *The Winter Annual Meeting of the ASME Winter Annual Meeting 6th Annual Symposium on Haptic Interfaces for Virtual Environments and Teleoperation Systems, ASME International Mechanical Engineering Congress and Exposition(IMECE97)*, pp. 115-122, 1997.

[9] Y. Tsumaki, H. Naruse, D.N. Nenchev, and M. Uchiyama, "Design of a compact 6-dof haptic interface," *Proceedings of the 1998 IEEE International Conference on Robotics and Automation*, pp. 2580-2585, 1998.

[10] K.Y. Woo, B.D. Jin, and D.S. Kwon, "A 6 DOF force-

reflecting hand controller using the fiverbar parallel mechanism," *Proc. of IEEE International Conference on Robotics and Automation*, pp. 1597-1602, 1998.

[11] J.W. Yoon and J. Ryu, "Analysis and design of a new haptic device using a parallel mechanism," *Journal of Control, Automation and Systems Engineering*, vol. 7, no.1, pp. 32-40, 2001.

[12] C. Gosselin and J. Angeles, "Singularity analysis of closed-loop kinematic chains," *IEEE Transactions on Robotics and Automation*, vol. 6, pp. 281-290, 1990.

[13] R.E. Stamper, "A three degree of freedom parallel mnipulator with only translation degree of freedom." Ph.D Thesis, University of Maryland, Dept. Of Mech. Eng. and Institute for systems Research, 1997.

[14] O. Ma and J. Angeles, "Architecture singulrarities of platform manipulators," *Proc. IEEE International Conference on Robotics and Automation*, pp. 1542-1547, 1991.

[15] C.L. Collins, "Singularity analysis and design of parallel manipulators," Ph.D Thesis, University of California, Irvine, Dept. of Mechanical and Aerospace Engineering, 1997.

[16] C. Reboulet and S. Leguay-Durand, "The interest of redundancy for the design of a spherical parallel manipulator," *5th International Workshop on Advances in Robotic Kinematics*, pp. 369-378, 1996.

[17] S.J. Ryu, J.W. Kim, and F.C. Park, "Eclipse: an overactuated parallel mechanism for rapid machining", *ASME International Mechanical Engineering Congress and Exposition*, vol.8, pp.681-689, 1998.

[18] J.F O'Brien and J.T. Wen, "On kinematic instability of parallel robot," *Proceedings of the 2nd Workshop on Computational kinematics*, pp. 279-290, 2001.

[19] C. Gosselin and J. Wang, "Static balancing of spatial six-degree-of freedom parallel mechanisms with revolute actuators." *Journal of Robotic System*, vol.17, no.3, pp. 159-170, 2000.

[20] Hunt, K. H., "Kinematic geometry of mechanisms." Oxford, UK., Oxford Science Publication., 1978

Young-Hoon Chung
received the B.S. degree in mechanical engineering and the M.S. degree in the mechanical enginee-ring, both from Yeungnam University, Gyoung-San, Korea, in 1997 and 1999, respectively, where he is currently a Ph.D candidate. His research interests are focused on the design of haptic device with parallel mechanisms, haptic rendering and singularity analysis of parallel manipulators.

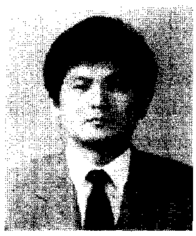

Jaewon Lee
received the B.S. degree in mechanical engineering from Seoul National University, Seoul, Korea, in 1979 and the M.S degree in mechanical engineering from the Korean Advanced Institute of Science and Technology, in 1981 and the Ph.D degree in mechanical engineering from the Georgia Institute of Technology, USA., in 1990. He is a Professor in the School of Mechanical Engineering, Gyoung-San, Korea, where he joined the faculty in 1991. His research interests are in the control of flexible structure, parallel manipulator, haptic device and teleoperation for position and force control.